

Prediction models of dye adsorption by *Treptacantha barbata*

Treptacantha barbata'nın boya adsorpsiyonunun tahmin modellemeleri

Esra Üçüncü Tunca¹ • Pınar Akdoğan Şirin^{2*} • Hasan Türe³

¹ Dolunay Mah. Fikir Sok., 52400 Fatsa, Ordu, Türkiye

² Ordu University, Fatsa Faculty of Marine Science, Department of Fisheries Technology Engineering, 52400, Ordu, Türkiye

³ Ordu University, Fatsa Faculty of Marine Science, Department of Marine Science and Technology Engineering, 52400 Fatsa, Ordu, Türkiye

 <https://orcid.org/0000-0002-9024-8477>

 <https://orcid.org/0000-0001-8518-0044>

 <https://orcid.org/0000-0003-4883-0751>

*Corresponding author: pinarakdogansirin@odu.edu.tr

Received date: 28.06.2022

Accepted date: 31.08.2022

How to cite this paper:

Üçüncü Tunca, E., Akdoğan Şirin, P., & Türe, H. (2022). Prediction models of dye adsorption by *Treptacantha barbata*. *Ege Journal of Fisheries and Aquatic Sciences*, 39(4), 300-310. DOI: 10.12714/egejfas.39.4.05

Abstract: This study's objective was to develop a model to determine dye adsorption efficiency of *Treptacantha barbata* (Stackhouse) Orellana & Sansón, 2019 (formerly *Cystoseira barbata* (Stackhouse) C. Agardh, 1820). During the experiments, treatment groups, such as initial dye Methylene Blue (MB) concentration (0.1-10.0 mg L⁻¹), contact time (5 to 1440 min) and adsorbent dosage (0.1-2 g) were applied. Scanning electron microscopy, energy dispersive X-ray, and Fourier Transform Infrared Spectroscopy were used to analyze the adsorbent. *T. barbata* was found to be quite successful in removing dye (69% -100%) for all experiments, and the *q_e* values increased with the increased the initial dye concentration. Very rapid dye removal was detected during the first contact time, especially up to 15 min. Isotherms, kinetics, and regression models were applied to the batch experimental results. The results displayed that adsorption process was suitable with the Langmuir isotherm model (R²: 0.97).

Keywords: Adsorption, isotherm models, regression, *Treptacantha barbata*

Öz: Bu çalışmanın amacı, *Treptacantha barbata* (Stackhouse) Orellana & Sansón, 2019 (önceki ismi ile *Cystoseira barbata* (Stackhouse) C. Agardh, 1820) boya adsorpsiyon etkinliğini araştırmak ve modellemektir. Deneyler, başlangıç Metilen Mavisi boya konsantrasyonu (0,1-10,0 mg L⁻¹), temas süresi (5- 1440 dakika) ve adsorban dozu (0,1-2 g) gibi parametrelere göre tasarlanmıştır. Adsorban, taramalı elektron mikroskobu-enerji dağılımlı X-ışını ve Fourier Dönüşümü Kızılötesi Spektroskopisi ile karakterize edilmiştir. *T. barbata* tüm deney gruplarında boya gideriminde (%69-100) oldukça başarılı bulunmuş ve *q_e* değerleri başlangıç boya konsantrasyonundaki artışa paralel olarak artmıştır. İlk temas süresinde, özellikle 15 dakikaya kadar boyanın çok hızlı uzaklaştırıldığı tespit edilmiştir. Kesikli deneysel verilere izoterm, kinetik ve regresyon modelleri uygulanmıştır. Sonuçlar, adsorpsiyon işleminin Langmuir izoterm modeliyle (R²: 0.97) iyi bir şekilde uyduğunu ortaya koymuştur.

Anahtar kelimeler: Adsorpsiyon, izoterm modelleri, regresyon, *Treptacantha barbata*

INTRODUCTION

Recently, the importance of sustainable and renewable systems has been increasing order to overcome the increasing environmental problems. Especially, the removal of contaminants from the environment has gained great importance, and different treatment methods such as ion exchange, membrane separation, electrochemical treatment, ozonation, chemical reduction, and microbial treatment have been developed for their removal (Jerold and Sivasubramanian 2016; Amin et al., 2020; Hamouda et al., 2020; Renita et al., 2021; Soto-Ramirez et al., 2021).

Owing to its affordable price and high effectiveness, the adsorption technique is more popular than other methods. (Marzbali et al., 2017; Jafari et al., 2020), versatility and reversibility (Hannachi and Hafidh, 2020), non-toxic and environmentally friendly properties (Radoor et al., 2020; Joshiba et al., 2021). The adsorption based on the process of pulling based liquid mixture in the environment to the solid

surface by chemical or physical bonds (Al-Ghouthi and Da'ana, 2020). The unbalanced forces of the atoms on adsorbent attract adsorbent in solution to the solid surface and balance the surface forces. In this way, the adsorption of the contaminant in the solution onto the solid surface occurs. In the adsorption process, biological agents such as algae and bacteria are used (living or dead forms) (Giannakoudakis et al., 2018; Majhi and Patra, 2020; Venkataraghavan et al., 2020), as well as biopolymers like alginate (Üçüncü Tunca et al., 2017; Vu et al., 2017; Xia et al., 2018) are developed as adsorbents. Research continues to find new, inexpensive, and efficient adsorbents for removing dye and metal ions from wastewater.

Marine macroalgae, also called seaweeds, are the primary producers in marine ecosystems. The ability of algae to absorb pollutants from the environment has enabled them to be accepted as pioneers (Priyadarshini et al., 2019) and they are

thought to exhibit highly dominant adsorption behavior (Jerold and Sivasubramanian 2016; El-Naggar et al., 2021). In addition to their efficient adsorption capabilities, they are preferred due to their non-toxic properties, widely distributed in nature (El Nemr et al., 2021a), eco-friendly and inexpensive production costs (El-Naggar et al., 2021). Macroalgae have important features like reuse of rich functional groups in the adsorption process. Hannachi and Hafidh (2020) revealed that the cell wall of brown macroalgae is generally consisting of sulfated fucoidans (polysaccharides), cellulose, alginates and researchers stated that this situation is important in binding the pollutants.

Macroalgae are considered suitable organisms for organic bio-sorption because they contain different anionic active regions that is hydroxyl, carboxyl, amine, and phosphate in structure of their cell walls (Daneshvar et al., 2017; El-Naggar et al., 2021). The sorption capacity of each macroalgae varies because these active regions differ depending on the macroalgae species. Simultaneously, the type of pollutant that macroalgae is exposed to can affect the success of removal. Researchers have looked at the ability of macroalgae to remove a variety of pollutants, containing heavy metals and dyes with various characteristics. (Essekri et al., 2020; Mahajan and Kaushal, 2020; Mahini et al., 2018; Omar et al., 2018; Filote et al., 2019; Lebron et al., 2021). These synthetic dyes, used in many sectors like cosmetics, food, paper, and textiles (Lyra et al., 2009; Mohammed and Mabrouk, 2020), pollute the aquatic environment and can form dangerous derivatives after being metabolized (Bouzikri et al., 2020). Furthermore, it is stated that the accumulation of these dyes in aquatic systems may reduce the amount of dissolved oxygen due to the reduction of light transmittance and this may cause the extinction of living things (Lebron et al., 2021). Methylene blue (MB), which was utilized as a contaminant in this work, is a cationic synthetic dye having toxic effects such as teratogenicity, mutagenicity, neurotoxicity, and nucleic acid damage (Ghosh et al., 2021). It is used for treating methemoglobinemia (Cefalu et al., 2020; Radoor et al., 2020), treating fish diseases in aquaculture (Xu et al., 2012; Lv et al., 2018; Xu et al., 2019) and as a colorant in the textile industry (Deng et al., 2011; Ait Ahsaine et al., 2018; Hasan et al., 2020).

In this research, the removal efficiency of *T. barbata* was evaluated for cationic MB dye, and the adsorption process was modeled using regression analysis. The impact of some variables such as, initial dye level (mg L^{-1}), contact time (min), and bio-sorbent mass (g) was investigated. The various kinetic models and equilibrium isotherm models were investigated to explain the mechanism of removal of MB. Fourier Transform Infrared Spectroscopy (FT-IR analysis) was used to determine the interaction between the functional groups of the macroalgae surface and dye molecules. Scanning electron microscopy–energy dispersive X-ray (SEM-EDX) was also used to investigate the morphology and surface characteristics.

MATERIAL AND METHODS

Chemicals and adsorbent preparation

Methylene Blue (MB) (molecular formula: $\text{C}_{16}\text{H}_{18}\text{ClN}_3\text{S}$ and molecular weight: $319.85 \text{ g mol}^{-1}$) was obtained from Pancreac®. A stock solution (1000 mg L^{-1}) of MB was prepared by dilution.

Treptacantha barbata (brown marine algae) biomasses were collected from the coast of the Black Sea (Ordu, Türkiye) ($41^\circ 12'61'' \text{ N}$; $37^\circ 69' 28'' \text{ E}$). The samples brought to the laboratory where washed to remove impurities. Macroalgae samples were first sun-dried for 96 hours and then in the oven at 60°C for 24 hours (Vijayaraghavan et al., 2016). Dry biomass was ground and sieved through a $941 \mu\text{m}$ mesh sieve.

Characterization of adsorbents

The FT-IR spectrometer (Bruker Tensor 27) was utilized to determine the functional groups on the *T. barbata* surface. The morphology and adsorbent surface composition was investigated using a scanning electron microscope (Hitachi SU 1510).

Sorption experiments

A series of batch tests with three replicates were performed to search *T. barbata*'s ability to adsorb MB. ($T: 25 \pm 2$, $\text{pH}: 9.2-9.5$). The adsorption process was studied with several initial dye concentrations ($0.5, 1.0, 2.0, 5.0, \text{ and } 10 \text{ mg L}^{-1}$), contact time (5 to 1440 min), and adsorbent dosage ($0.1 \text{ to } 2.0 \text{ g}$) to find the effect of sorption conditions on MB removal.

The desired dye concentrations were obtained from the stock solution and 100 mL of solution was added into 250 mL conical flasks. First, a calibration curve was formed and the test concentrations were determined accordingly (R^2 value: 0.9991).

The test flasks were located in a shaking incubator (WiseCube, Precise Shaking Incubator, BenchTop Type (WIS-20R) at 80 rpm during the experiment. According to the determined contact times, 2 mL samples from the supernatant part of the test groups were taken into centrifuge tubes. The suspended materials were centrifuged for 5 min at 1000 rpm and the number of MB concentrations were analyzed at 664 nm respectively utilizing a UV-Vis Spectrophotometer (Shimadzu-UVmini-1240).

Using the following equations, MB removal effectiveness and adsorption capacity were estimated. (Naushad et al., 2015; Zhang et al., 2016; Broujeni et al., 2021; Renita et al., 2021).

$$q_e = \frac{(C_0 - C_e)}{m} \times V$$

$$R \% = \frac{C_0 - C_e}{C_0} \times 100$$

Where q_e (mg g^{-1}) demonstrates the equilibrium adsorption capacity, $R\%$ is the removal efficiency of contaminant, C_0 and C_e (mg L^{-1}) are first and the equilibrium concentrations of MB, V (L) is the volume of test concentration, and m (g) is the dry weight of the adsorbent.

Adsorption isotherms

The adsorption isotherm models, such as Langmuir and Freundlich models were used to find the interactive mechanisms in the adsorption process. The adsorption isotherm equation of the Langmuir was applied in following equation: (Langmuir, 1916; Zhang et al., 2016; El Nemr et al., 2021b).

$$\frac{C_e}{q_e} = \frac{1}{q_{max}b} + \frac{1}{q_{max}}$$

Where q_e (mg g^{-1}) represents dye level at the equilibrium on the adsorbent, C_e (mg L^{-1}) is the equilibrium concentration of dye in solution, b is the Langmuir constant, and q_{max} is the monolayer adsorption capacity (mg g^{-1}).

The Freundlich model applies to heterogeneous surfaces and uses the equation below: (Abdelhameed et al., 2020).

$$\ln q_e = \ln K_f + \frac{1}{n} \ln C_e$$

where K_f (L mg^{-1}) and n are constants that define the adsorption capacity and intensity, respectively. q_e and C_e are previously defined.

Statistical analysis

Regression analysis was applied to the prediction models of the adsorption data. The most suitable regression models for the data were selected and presented, considering the R^2 values. All statistical calculations were made using SPSS 21.0 software (IBM, Portsmouth, UK).

RESULTS AND DISCUSSION

Several physicochemical processes such as initial concentration, pH, time, etc. have an impact on the adsorption process (Broujeni et al., 2021). In this work, in which the adsorption efficiencies of MB concentrations by *T. barbata* were examined; the effects of contact time, initial dye concentration, and adsorbent concentration were studied. In the experiments, it was found that there was no dye precipitation in the test groups, and *T. barbata* was found to be quite successful in removing MB at tested concentrations. Adsorption isotherms were formed and dye removal estimation models were performed using regression analysis. Control groups were also studied under the same conditions as all test groups to determine the amount of precipitation. It was determined that the control group containing only adsorbent did not statistically affect the results of the experimental groups.

Characterization of adsorbent

The surface structural features of *T. barbata* were examined before and after the adsorption of MB using SEM. Samples were coated with gold. The surface images of the prepared samples were analyzed at different magnifications (x650, x1000, x4000). The control group and the samples exposed to dye molecules showed different surface properties. As seen in Figure 1a, the surface of raw macroalgae has a bumpy structure with prominent pits. However, the depths of the pits on the macroalgae surfaces were considerably decreased after the adsorption process (Figure 1b) suggesting that the biomass surfaces appear to be covered by methylene blue dye. These results were similar to those observed by Koyuncu and Kul (2020), who reported that non-living lichen (*Pseudevernia furfuracea* (L.) Zopf.) surfaces were covered with the adsorption of MB dye.

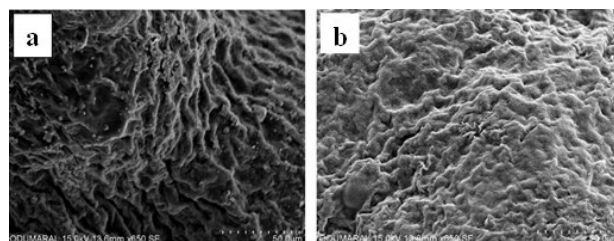


Figure 1. SEM images of *T. barbata* (a) before adsorption of MB, (b) after adsorption of MB

EDX analysis was used to investigate the distribution of various elements in the biomass. There are active negative functional groups on algae sorbents and they are suitable for the adsorption of molecules with cationic properties (Abdelhameed et al., 2020). EDX results indicated various elements containing carbon (C), oxygen (O), potassium (K^+), magnesium (Mg^{+2}), sulfur (S) and chlorine (Cl). S, Cl, Na, and P were eliminated after dye interactions between macroalgae and MB dye. These elements tend to create negative charges, and this decrease could be described by the interaction of the cationic dye with macroalgae (Figure 2). The FT-IR spectra of raw and MB biosorbed *T. barbata* were investigated to gain a better understanding of the intensity and kind of functional groups on the biomass surface. The FT-IR spectra of the raw *T. barbata* biomass with and without dye-loaded are demonstrated in Figure 3. Figure 3 shows the infrared spectrum of pure algae, which shows a variety of absorption peaks, suggesting its complexity. Various bands were detected at 3281 cm^{-1} ($-\text{OH}$ or $-\text{NH}_2$), 2922 cm^{-1} ($-\text{CH}$ or COOH), 1613 cm^{-1} ($>\text{C}=\text{O}$), 1414 cm^{-1} (aromatic ring), 1247 cm^{-1} ($\text{C}-\text{O}$) and 1024 cm^{-1} ($\text{C}-\text{O}$ or $>\text{S}=\text{O}$) (El Jamal and Ncibi, 2012). Identical spectra were reported in the literature from other algae such as *C. barbata*, and *C. baccata* (Caparkaya and Cavas 2008; Lodeiro et al., 2006). When the biomass was loaded with the dye ion, there were some changes in the distance between these peaks, leading to the conclusion that carboxyl groups were primarily involved in dye absorption.

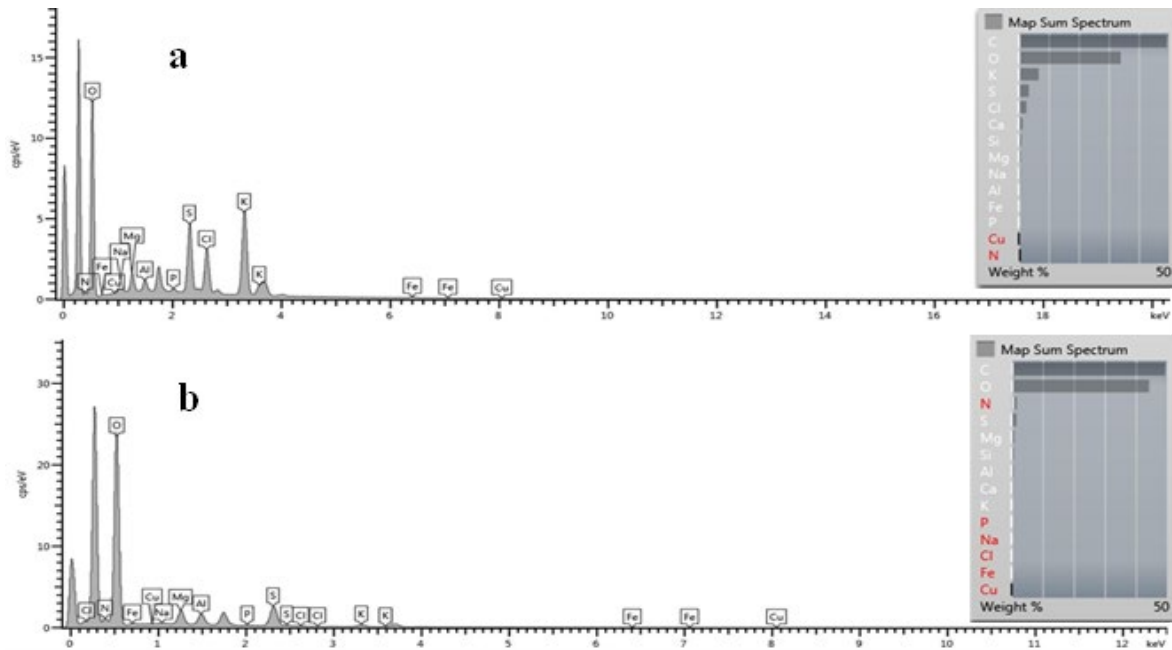


Figure 2. EDX spectrum of algal biomass (a) and MB+algal biomass (b)

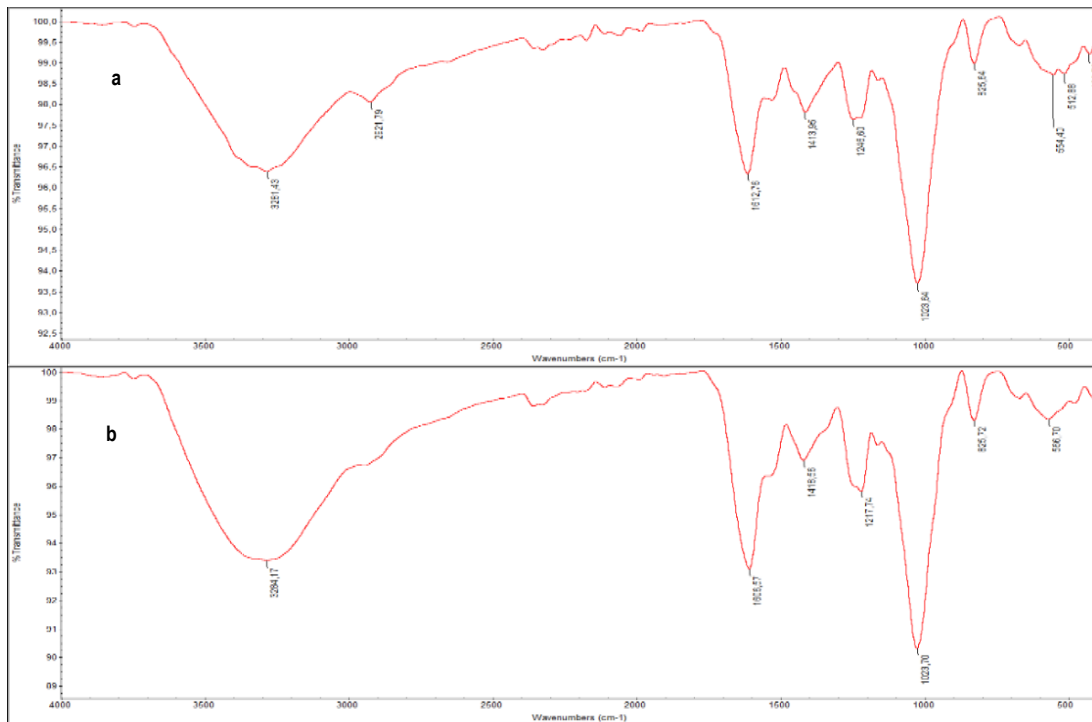


Figure 3. FT-IR spectra of algal biomass (a) and MB+algal biomass (b)

Prediction models

Regression analysis was done to compare the modeled adsorption in the medium and to observe any potential correlations or differences depending on the time. Time-dependent, adsorbent dosage-dependent and

initial concentration-dependent estimation models were examined, and all regression models (linear, cubic, logarithmic, etc.) were applied. The most suitable models were selected on the basis of R² values (R² > 0.8).

Prediction models of initial concentration effect on adsorption

The adsorption efficiencies of *T. barbata* were investigated using five initial concentrations of MB dye (0.5, 1.0, 2.0, 5.0, and 10.0 mg L⁻¹) at room temperature (25 ± 2 °C), pH 9.2–9.5 (Figure 4). The effects of 9 different contact times (5, 15, 30, 45, 60, 120, 240, 480, and 1440 min) were also studied on MB adsorption by macroalgae for each concentration applied.

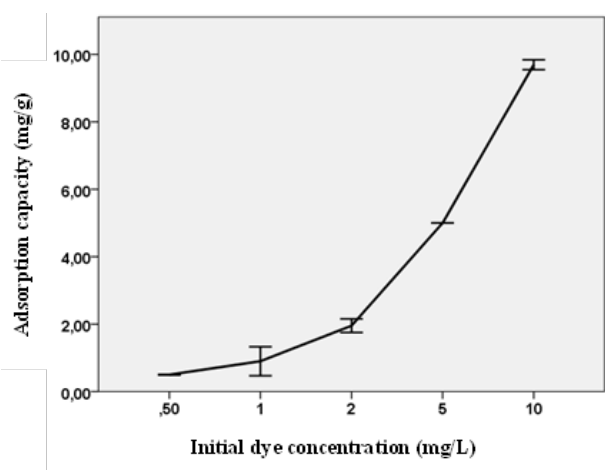


Figure 4. Effect of initial MB concentration on adsorption capacity (24 h)

The maximum dye adsorption capacity of macroalgae was found as 9.70 mg g⁻¹ for the applied concentration. The q_e values increased in parallel with the increment in the primary dye availability, as in many studies in the literature (Mahajan and Kaushal, 2020; El Nembr et al., 2021b). This indicates presence of an interaction between the applied cationic dye and macroalgae (Bouzikri et al., 2020). Increasing the amount of adsorbents in the medium also increases the possibility of adsorbents and sorbent binding or collision (Sun et al., 2019; Radwan et al., 2020). However, the increase in the concentration decreases the mass transfer resistance of the adsorptive, and therefore adsorptive uptake increases (Melo et al., 2018; Radwan et al., 2020).

Some studies have shown that metal adsorption rates increase owing to the increase in the initial level (Sun et al., 2019; Hamouda et al., 2020; Ghosh et al., 2021). It has also been determined that the removal efficiency of different dyes or metal ions, increases with increasing concentration, but this increase was determined to be in small quantities (Hamouda et al., 2020). In this study, it was seen that with the increase in the initial dye level, removal percentages gradually decreased, similar to some studies in Figure 5. (Renita et al., 2021; El Nembr et al., 2021b). This decrease tends to increase again after reaching a certain concentration. Furthermore, when the initial concentration-dependent removal efficiencies were investigated, it was determined that the highest adsorption rates were concentrated in the lower initial concentration groups (Figure 5).

Despite the high removal rates, a tendency to decrease in efficiency was observed in groups up to 2 mg L⁻¹. At low

concentrations, the presence of more binding sites than the dye molecule in the solution may have increased the efficiency (Renita et al., 2021). The reason for this sharp decrease trend may be due to the fact that the dye molecules where the amount increases in solution cannot find enough surface area to bind (Husien et al., 2019). These results supported each other with the regression results. Figure 6 shows the regression models of the change in removal efficiencies relative to the initial concentration (R^2 : 0.869–0.998 except at 120 min). It was determined that other groups, except for 120 min, 480 min, and 1440 min, formed quite similar trends. The decrease-increase movements stand out in the efficiency of removal depending on the initial concentration. In groups with similar trends, it is anticipated that the initial declining trend will tend to increase after about 3 mg L⁻¹ and then decrease after 8 mg L⁻¹. In 120 min model, the R^2 value was determined as 0.542 and it showed a different lighter decrease-increase profile than the other groups. The 120 min regression modeling was not used in the article due to its low R^2 value (0.542). It is thought that the adsorption will reach equilibrium after 60 min, and it may have become more stable after 120 min.

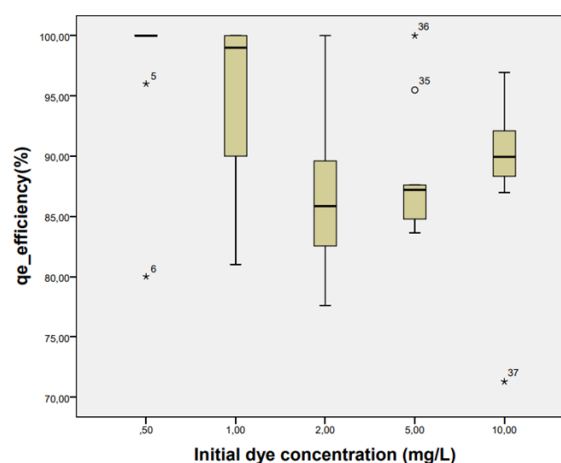


Figure 5. Effect of initial concentration on the MB adsorption efficiency by *T. barbata*

Prediction models of contact time on adsorption

Adsorption efficiencies of *T. barbata* according to the exposure time to the cationic dye MB were also investigated. The effect of contact time on the adsorption process was investigated at different time intervals (5 to 1440 min). Figure 7 illustrates the evolution of the adsorption of MB by *T. barbata* for different contact times. It shows that MB adsorption tends to increase with time, although it makes an insignificant number of increase-decrease movements, and it reaches equilibrium after 500 min. After equilibrium, it was determined that there was a very small amount or no adsorption. Studies have suggested that sorption efficiencies increase depending on the contact time until equilibrium (Nasoudari et al., 2020). Contact time is a factor significantly affecting adsorption rates (Hannachi and Hafidh, 2020). When evaluated according to the removal percentages, very rapid dye removal (71.28%–100%) was detected during the first contact time (especially up to 15 min, Figure 8).

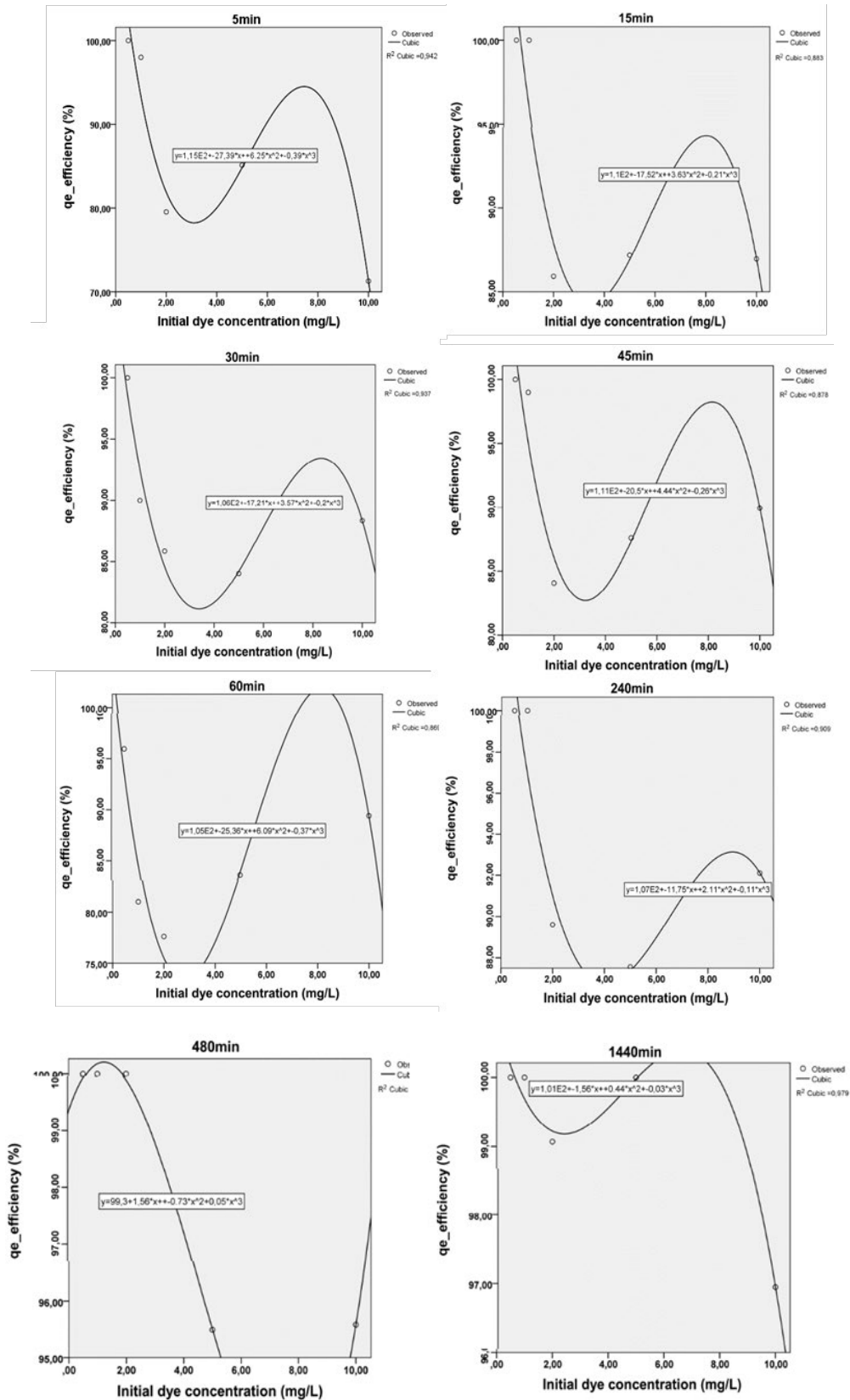


Figure 6. Prediction models of adsorption efficiency (initial dye concentration-dependent)

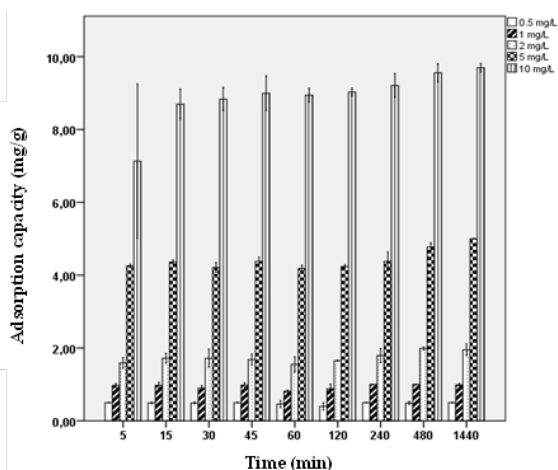


Figure 7. The effect of contact time on the MB adsorption capacity of *T. barbata*

As is known, there are some active binding sites on adsorbents (Abdelhameed et al., 2020). The reason for the rapid removal seen at the beginning of the experimental phase, may be due to the presence of these free active binding sites on the adsorbent (Ghosh et al., 2021; Mahajan and Kaushal 2020). It is thought that the reason why adsorption reached equilibrium may be the decrease in active binding sites on macroalgae over time (Sun et al., 2019) and the affinity of the adsorbant to the adsorbate may decrease. This saturation on the surface will decrease the driving force for removal (Mahajan and Kaushal 2020). Another reason may be the limitation of the mass transfer for the adsorbate molecules from the solution to the adsorbant surface (Broujeni et al., 2021). When all concentration groups were evaluated separately, the lowest adsorption percentages were 71.28% for 10 mg L⁻¹ (5 min), 79.54% (5 min) and 77.61% (60 min) for 2 mg L⁻¹. Notably, the 1 mg L⁻¹ groups showed a decrease-increase profile both positively and negatively over time and were more unstable than the other groups (Figure 8).

The lowest levels (0.5, 1.0 and 2.0 mg L⁻¹) showed similar time-dependent removal trend. In all groups, a decreasing trend was observed in the removal rates in 45 min. A smaller decrease-increase movement and a more stable profile were observed in the 5 and 10 mg L⁻¹ groups. The time-dependent regression models were formed. However, due to the increase-decrease trend observed in all groups, a suitable model could not be created for our data. Although models with an R² value above 0.8 were formed for some groups, when the models were examined, it was seen that the resulting peaks did not explain our data properly.

Effect of adsorbent dosage

Macroalgae dosage was applied in amounts varying from 0.1 to 2.0 g and removal efficiencies were determined after 45 min and 24 h. The other parameters were kept constant (T: 25 ± 2, pH:11.0, dye concentration: 2 mg L⁻¹).

The weight of the biosorbent in the medium is directly

related to availability of adsorption sites (Nasoudari et al., 2020) and affects the removal rates (Hannachi and Hafidh 2020). Some studies have determined an increase (El-Naggar et al., 2021; Radwan et al., 2020) or decrease (Tumin et al., 2008; Ghosh et al., 2021) in removal rates depending on the adsorbent dosage (Sun et al., 2019). The results may vary according to time, adsorbent, quantity, pH, T and the other parameters. In this study, both an increase and a decrease trend were observed (Figure 9). It is seen in the regression model that the removal rates increment with the increment in the amount of adsorbent, reaching their maximum value at about 1.5 g and then beginning to decrease slowly at 45 min. (Figure 9).

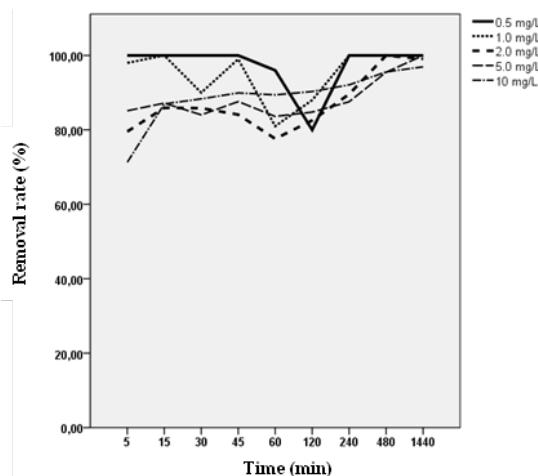


Figure 8. Time-dependent removal efficiencies of MB for all test groups

It is thought to be that the increase in the adsorbent in the medium also increases the adsorbent surface, thus providing more active binding sites for the dye (Sun et al., 2019; Melo et al., 2018; Radwan et al., 2020). The 24 h results showed an opposite trend of removal compared to the 45 min results. With the increase in the amount of the adsorbent, the removal efficiency tended to decrease, and it was observed that it reached equilibrium at a dose number of approximately 1.5 g. The possibility of aggregation will occur with increasing time in high adsorbent amounts (El-Naggar et al., 2021). In addition, it is thought that this situation will decrease the surface area and hence reduce the adsorption efficiency (Karthikeyan et al., 2007; Tural et al., 2017; Silva et al., 2019; Ghosh et al., 2021). This may explain the decrease in efficiency seen in the high number of adsorbents in our data. Parameters such as the surface area of the adsorbent, particle size, and temperature are among the factors affecting the adsorption efficiency. Under suitable conditions, the width of the surface area is directly proportional to the molecular retention capacity of the adsorbent surface (Weber, 1972; El-Naggar et al., 2021). In this context, with the addition of the adsorbent to the adsorption process in smaller pieces, the number of molecules to be held on the unit surface will increase. It is thought that the fact that macroalgae were used in small pieces in this study may have increased the efficiency of adsorption.

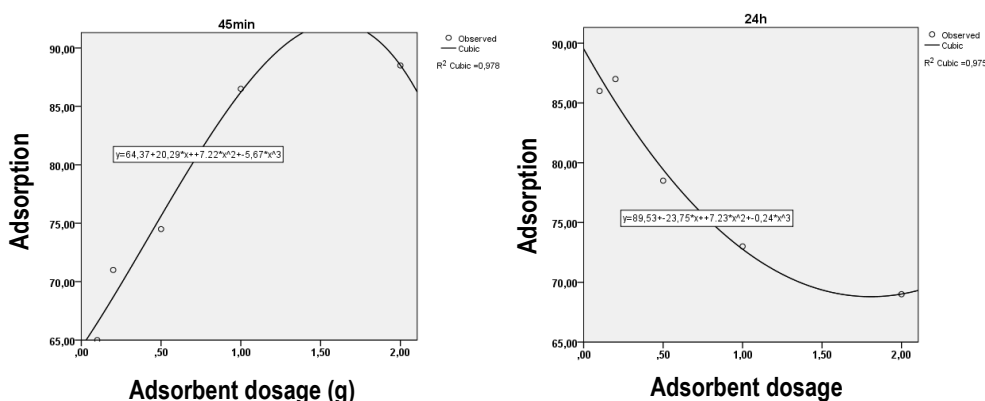


Figure 9. Prediction models (adsorbent dosage-dependent)

Adsorption isotherm study

The isotherm models of Langmuir and Freundlich were used to examine the removal process of MB dye by *T. barbata*. The corresponding parameters of the models and the fitted equilibrium data are shown in Table 1. Results indicated that the Langmuir model described adsorption more accurately than the Freundlich model, with $R^2 > 0.97$. The fitting outcome is in line with the previous classification, which found that the majority of adsorption systems with a H type and subclass 2 curves exhibit good convergence with the Langmuir model (Giles et al., 1960).

As indicated in Table 1, the maximum adsorption capacity (Q_m) of *T. barbata* for the adsorption of MB dye was 73.53 mg g⁻¹. The maximum adsorption levels of some adsorbents for the adsorption of MB dyes from hydrated solutions are shown in Table 2. The data shown in Table 2 indicates that the Q_m of MB dyes on *T. barbata* is comparable to or higher than some other adsorbents. The essential characteristics of the Langmuir isotherm model can be given regarding the separation factor, R_L , as in the equation given below: (Soltani et al., 2014)

$$R_L = \frac{1}{1 + C_0 K_L}$$

where C_0 (mg L⁻¹) is the first metal ion density and K_L (L mg⁻¹) is the Langmuir constant. The values of R_L parameters are considered $R_L = 0, 0 < R_L < 1$ and $R_L > 1$ which shows that adsorption is unchangeable, suitable, and unsuitable, respectively. The values of the R_L demonstrated in Table 1 indicate that R_L is from 0.580 to 0.933; therefore, the adsorption of MB dyes onto *T. barbata* would be suitable.

Table 1. Langmuir and Freundlich adsorption isotherm details for MB adsorption on *T. barbata*

Q_{exp} (mg g ⁻¹)	Isotherm models	Parameters	
92.41	Langmuir	R^2	0.97
		Q_{max} (mg g ⁻¹)	73.53
		K_L (L mg ⁻¹)	0.072
	Freunlich	R_L	0.580-0.933
		R^2	0.95
	K_F (L g ⁻¹)	6.92	
	n	0.819	

Table 2. Maximum adsorption capacity of some adsorbents for MB removal from aqueous solution

Adsorbent	Q_m (mg g ⁻¹)	Reference
Modified ball clay	100	Auta and Hameed, 2012
Iron-tannic acid (TA) complexes	67.41	Li et al., 2016
Halloysite nanotubes	40.82	Zhao and Liu, 2008
TA-modified Fe3O4 nanoparticles	90.90	Abkenar et al., 2015
Cellulose nanocrystals	118	Batmaz et al., 2014
Rice husk	8.07	Shih, 2012
Multi-walled carbon nanotubes	119	Shahryari et al., 2010
NaOH-treated waste activated sludge	53.7	Gobi et al., 2011
Natural Jordanian Tripoli	16.6	Alzaydien, 2009
<i>T. barbata</i>	73.53	This work

CONCLUSION

Removal efficiency of MB dye by *T. barbata* was evaluated according to dissimilar parameters (contact time, adsorbent dosage, and initial dye concentration). The process of dye adsorption was modeled using regression analysis and adsorption isotherms. The algal biomass was investigated by SEM-EDX and FT-IR before and after treatment. According to the results, very rapid dye removal (71.28%-100%) was detected during the first contact time (up to 15 min). The highest adsorption rates were determined in lower initial concentration groups because of the presence of more binding sites. The decrease-increase movements were observed in the removal efficiency depending on the initial concentration and the contact time until equilibrium was reached. Regression models showed that the removal rates increment with the increment in the amount of adsorbent, reaching the maximum value at about 1.5 g and then begin to decrease slowly. The Langmuir isotherm seemed to be the super fitted model for all the experimental data. These results indicated that the *T. barbata* surface had monolayer and homogenous properties. In conclusion, it was considered that *T. barbata* was a useful and efficient adsorbent for the removal process. It is thought that *T. barbata* may be preferred as an alternative sorbent to be used in treatment studies due to its advantages such as convenient adsorptive properties, being inexpensive, and being eco-friendly.

ACKNOWLEDGEMENTS AND FUNDING

This research has not received a specific grant, fund or other support from any funding agency in the public, commercial, or not-for-profit sectors.

AUTHORSHIP CONTRIBUTIONS

The experiments were designed by Esra Üçüncü Tunca. Laboratory studies were carried out by Pınar A. Şirin. Adsorption isotherm models were interpreted by Hasan Türe. The article was written by all researchers.

CONFLICT OF INTEREST

The authors no conflict of interest to declare.

ETHICS APPROVAL

No specific ethical approval was necessary for this study.

DATA AVAILABILITY

For questions regarding datasets, the corresponding author should be contacted.

REFERENCES

- Abdelhameed, R.M., Alzahrani, E., Shaltout, A.A., & Moghazy, R.M. (2020). Development of biological macroalgae lignins using copper based metal-organic framework for selective adsorption of cationic dye from mixed dyes. *International Journal of Biological Macromolecules*, 165, 2984–2993. DOI: [10.1016/j.jbiomac.2020.10.157](https://doi.org/10.1016/j.jbiomac.2020.10.157)
- Abkenar, S.D., Khoobi, M., Tarasi, R., Hosseini, M., Shafiee, A., & Ganjali, M.R. (2015). Fast removal of methylene blue from aqueous solution using magnetic-modified Fe₃O₄ nanoparticles. *Journal of Environmental Engineering and Science*, 141 (1), 04014049. DOI: [10.1061/\(ASCE\)EE.1943-7870.0000878](https://doi.org/10.1061/(ASCE)EE.1943-7870.0000878)
- Ait Ahsaine, H., Zbair, M., Anfar, Z., Naciri, Y., El Haouti, R., El Alem, N., & Ezahri, M. (2018). Cationic dyes adsorption onto high surface area 'almond shell' activated carbon: Kinetics, equilibrium isotherms and surface statistical modeling. *Materials Today Chemistry*, 8, 121-132. DOI: [10.1016/j.mtchem.2018.03.004](https://doi.org/10.1016/j.mtchem.2018.03.004)
- Al-Ghouti, M.A., & Da'ana, D.A. (2020). Guidelines for the use and interpretation of adsorption isotherm models: A review. *Journal of Hazardous Materials*, 393, 122383. DOI: [10.1016/j.jhazmat.2020.122383](https://doi.org/10.1016/j.jhazmat.2020.122383)
- Alzaydien, A., S. (2009). Adsorption of methylene blue from aqueous solution onto a low-cost natural Jordanian Tripoli. *American Journal of Applied Sciences*, 5 (3):197-208.
- Amin, M.T., Alazba, A.A., & Shafiq, M. (2020) Comparative removal of lead and nickel ions onto nanofibrous sheet of activated polyacrylonitrile in batch adsorption and application of conventional kinetic and isotherm models. *Membranes (Basel)*, 11 (1). DOI: [10.3390/membranes11010010](https://doi.org/10.3390/membranes11010010)
- Auta, M., & Hameed, B.H. (2012). Modified mesoporous clay adsorbent for adsorption isotherm and kinetics of methylene blue. *Chemical Engineering Journal*, 198-199, 219-227. DOI: [10.1016/j.cej.2012.05.075](https://doi.org/10.1016/j.cej.2012.05.075)
- Batmaz, R., Mohammed, N., Zaman, M., Minhas, G., Berry, M.R., & Tam, K.C. (2014). Cellulose nanocrystals as promising adsorbents for the removal of cationic dyes. *Cellulose* 21 (3), 1655-1665. DOI: [10.1007/s10570-014-0168-8](https://doi.org/10.1007/s10570-014-0168-8)
- Bouzikri, S., Ouasfi, N., Benzidia, N., Salhi, A., Bakkas, S., & Khamliche, L. (2020). Marine alga "*Bifurcaria bifurcata*": biosorption of Reactive Blue 19 and methylene blue from aqueous solutions. *Environmental Science and Pollution Research*, 27 (27), 33636-33648. DOI: [10.1007/s11356-020-07846-w](https://doi.org/10.1007/s11356-020-07846-w)
- Broujeni, B.R., Nilchi, A., & Azadi, F. (2021). Adsorption modeling and optimization of thorium (IV) ion from aqueous solution using chitosan/TiO₂ nanocomposite: Application of artificial neural network and genetic algorithm. *Environmental Nanotechnology, Monitoring & Management*, 15, 100400. DOI: [10.1016/j.enmm.2020.100400](https://doi.org/10.1016/j.enmm.2020.100400)
- Caparkaya, D., & Cavas, L. (2008). Biosorption of Methylene Blue by a Brown Alga *Cystoseira barbatula* Kützting. *Acta Chimica Slovenica*, 55 (3).
- Cefalu, J.N., Joshi, T.V., Spalitta, M.J., Kadi, C.J., Diaz, J.H., Eskander, J.P., Cornett, E.M., & Kaye, A.D. (2020). Methemoglobinemia in the operating room and intensive care unit: Early recognition, pathophysiology, and management. *Advances in Therapy*, 37 (5): 1714-23. DOI: [10.1007/s12325-020-01282-5](https://doi.org/10.1007/s12325-020-01282-5)
- Daneshvar, E., Vazirzadeh, A., Niazi, A., Sillanpää, M., & Bhatnagar, A. (2017). A comparative study of methylene blue biosorption using different modified brown, red and green macroalgae—Effect of pretreatment. *Chemical Engineering Journal*, 307, 435-446. DOI: [10.1016/j.cej.2016.08.093](https://doi.org/10.1016/j.cej.2016.08.093)
- Deng, H., Lu, J., Li, G., Zhang, G., & Wang, X. (2011). Adsorption of methylene blue on adsorbent materials produced from cotton stalk. *Chemical Engineering Journal*, 172(1), 326-334. DOI: [10.1016/j.cej.2011.06.013](https://doi.org/10.1016/j.cej.2011.06.013)
- El Jamal, M.M., & Ncibi, M.C. (2012). Biosorption of methylene blue by chaetophora elegans algae: Kinetics, equilibrium and thermodynamic studies. *Acta Chimica Slovenica*, 59 (1), 24-31.
- El-Naggar, N.E., Hamouda, R.A., Saddiq, A.A., & Alkinani, M.H. (2021). Simultaneous bioremediation of cationic copper ions and anionic methyl orange azo dye by brown marine alga *Fucus vesiculosus*. *Scientific Reports*, 11 (1): 3555. DOI: [10.1038/s41598-021-82827-8](https://doi.org/10.1038/s41598-021-82827-8)
- El Nemr, M.A., Ismail, I.M., Abdelmonem, N.M., El Nemr, A., & Ragab, S. (2021a). Amination of biochar surface from watermelon peel for toxic chromium removal enhancement. *Chinese Journal of Chemical Engineering*, 36, 199-222. DOI: [10.1016/j.cjche.2020.08.020](https://doi.org/10.1016/j.cjche.2020.08.020)
- El Nemr, A., Shoaib, A.G., El Sikaily, A., Mohamed, A.E.D.A., & Hassan, A.F. (2021b). Evaluation of cationic methylene blue dye removal by high surface area mesoporous activated carbon derived from *Ulva lactuca*. *Environmental Processes*, 8, 311–332. DOI: [10.1007/s40710-020-00487-8](https://doi.org/10.1007/s40710-020-00487-8)
- Essekri, A., Aarab, N., Hsini, A., Ajmal, Z., Laabd, M., El Ouardi, M., Abdelaziz, A.A., Rajae, L., & Albourine, A. (2020). Enhanced adsorptive removal of crystal violet dye from aqueous media using citric acid modified red-seaweed: experimental study combined with RSM process optimization. *Journal of Dispersion Science and Technology*, 1-14. DOI: [10.1080/01932691.2020.1857263](https://doi.org/10.1080/01932691.2020.1857263)
- Filote, C., Volf, I., Santos, S.C.R., & Botelho, C.M.S. (2019). Bioadsorptive removal of Pb(II) from aqueous solution by the biorefinery waste of *Fucus spiralis*. *Science of the Total Environment*, 648, 1201-1209. DOI: [10.1016/j.scitotenv.2018.08.210](https://doi.org/10.1016/j.scitotenv.2018.08.210)
- Ghosh, I., Sayanti, K., Chatterjee, T., Bar, N., & Das, S.K. (2021). Removal of methylene blue from aqueous solution using *Lathyrus sativus* husk: Adsorption study, MPR and ANN modelling. *Process Safety and Environmental Protection*, 149, 345-61. DOI: [10.1016/j.psep.2020.11.003](https://doi.org/10.1016/j.psep.2020.11.003)
- Giannakoudakis, D.A., Hosseini-Bandegharai, A., Tsafarakidou, P., Triantafyllidis, K.S., Kornaros, M., & Anastopoulos, I. (2018). *Aloe vera* waste biomass-based adsorbents for the removal of aquatic pollutants: A review. *Journal of Environmental Management*, 227, 354-364. DOI: [10.1016/j.jenvman.2018.08.064](https://doi.org/10.1016/j.jenvman.2018.08.064)
- Giles, C.H., Macewan, T.H., Nakhwa, S.N., & Smith, D. (1960). Studies in adsorption. Part XI. A system of classification of solution adsorption isotherms, and its use in diagnosis of adsorption mechanisms and in measurement of specific surface areas of solids, *Journal of the Chemical Society*, 3973–3993.

- Gobi, K., Mashitah, M.D., & Vadivelu, V.M. (2011). Adsorptive removal of Methylene Blue using novel adsorbent from palm oil mill effluent waste activated sludge: Equilibrium, thermodynamics and kinetic studies. *Chemical Engineering Journal*, 171 (3):1246-1252. DOI: [10.1016/j.cej.2011.05.036](https://doi.org/10.1016/j.cej.2011.05.036)
- Hamouda, R.A., El-Naggar, N.E.A., Doleib, N.M., & Saddiq, A.A. (2020). Bioprocessing strategies for cost-effective simultaneous removal of chromium and malachite green by marine alga *Enteromorpha intestinalis*. *Scientific Reports*, 10 (1), 1-19. DOI: [10.1038/s41598-020-70251-3](https://doi.org/10.1038/s41598-020-70251-3)
- Husien, S., Labena, A., El-Belely, E.F., Mahmoud, H.M., & Hamouda, A.S. (2019). Absorption of hexavalent chromium by green micro algae *Chlorella sorokiniana*: Live planktonic cells. *Water Practice and Technology*, 14 (3), 515-529. DOI: [10.2166/wpt.2019.034](https://doi.org/10.2166/wpt.2019.034)
- Hannachi, Y., & Hafidh, A. (2020). Biosorption potential of *Sargassum muticum* algal biomass for methylene blue and lead removal from aqueous medium. *International Journal of Environmental Science and Technology*, 17, 3875–3890. DOI: [10.1007/s13762-020-02742-9](https://doi.org/10.1007/s13762-020-02742-9)
- Hasan, I., Khan, R.A., Alharbi, W., Alharbi, K.H., Khanjer, M.A., & Alslame, A. (2020). Synthesis, characterization and photo-catalytic activity of guar-gum-g-alginate@ silver bionanocomposite material. *RSC Advances*, 10 (13), 7898-7911. DOI: [10.1039/D0RA00163E](https://doi.org/10.1039/D0RA00163E)
- Jafari, H., Mahdavinia, G.R., Kazemi, B., Javanshir, S., & Alinavaz, S. (2020). Basic dyes removal by adsorption process using magnetic *Fucus vesiculosus* (brown algae). *Journal of Water and Environmental Nanotechnology*, 5(3), 256-269. DOI: [10.22090/JWENT.2020.03.006](https://doi.org/10.22090/JWENT.2020.03.006)
- Jerold, M., & Sivasubramanian, V. (2016). Biosorption of malachite green from aqueous solution using brown marine macro algae *Sargassum swartzii*. *Desalination and Water Treatment*, 1-13. DOI: [10.1080/19443994.2016.1156582](https://doi.org/10.1080/19443994.2016.1156582)
- Joshiha, G.J., Kumar, P.S., Govarthanan, M., Nguenagni, P.T., Abilarasu, A., & Carolin, C.F. (2021). Investigation of magnetic silica nanocomposite immobilized *Pseudomonas fluorescens* as a biosorbent for the effective sequestration of Rhodamine B from aqueous systems. *Environmental Pollution*, 269, 116173. DOI: [10.1016/j.envpol.2020.116173](https://doi.org/10.1016/j.envpol.2020.116173)
- Karthikeyan, S., Balasubramanian, R., & Iyer, C.S. (2007). Evaluation of the marine algae *Ulva fasciata* and *Sargassum* sp. for the biosorption of Cu(II) from aqueous solutions. *Bioresource Technology*, 98 (2): 452-455. DOI: [10.1016/j.biortech.2006.01.010](https://doi.org/10.1016/j.biortech.2006.01.010)
- Koyuncu, H., & Kul, A.R. (2020). Removal of methylene blue dye from aqueous solution by nonliving lichen (*Pseudevernia furfuracea* (L.) Zopf.), as a novel biosorbent. *Applied Water Science*, 10 (2), 1-14. DOI: [10.1007/s13201-020-1156-9](https://doi.org/10.1007/s13201-020-1156-9)
- Langmuir, I. (1916). The constitution and fundamental properties of solids and liquids. *Journal of the American Chemical Society* 38: 2221–2295.
- Lebron, Y.A.R., Moreira, V.R., & de Souza Santos, L.V. (2021). Biosorption of methylene blue and eriochrome black T onto the brown macroalgae *Fucus vesiculosus*: equilibrium, kinetics, thermodynamics and optimization. *Environmental Technology*, 42 (2), 279-297. DOI: [10.1080/09593330.2019.1626914](https://doi.org/10.1080/09593330.2019.1626914)
- Li, Y.M., Miao, X., Wei, Z.G., Cui, J., Li, S.Y., Han, R.M., Zhang, Y., & Wei, W. (2016). Iron-tannic acid nanocomplexes: facile synthesis and application for removal of methylene blue from aqueous solution. *Digest Journal of Nanomaterials and Biostructures*. 11 (4): 1045-1061.
- Lodeiro, P., Barriada, J.L., Herrero, R., & De Vicente, M.S. (2006). The marine macroalga *Cystoseira baccata* as biosorbent for cadmium (II) and lead (II) removal: kinetic and equilibrium studies. *Environmental Pollution*, 142 (2), 264-273.
- Lv, X.M., Yang, X.L., Xie, X.Y., Yang, Z.Y., Hu, K., Wu, Y.J., Jiang, Y., Liu, T., Fang, W., & Huang, X.Y. (2018). Comparative transcriptome analysis of *Anguilla japonica* livers following exposure to methylene blue. *Aquaculture Research*, 49(3), 1232-1241. DOI: [10.1111/are.13576](https://doi.org/10.1111/are.13576)
- Lyra, E.S., Moreira, K.A., Porto, T.S., Carneiro da Cunha, M.N., Paz Júnior, F.B., Neto, B.B., Lima-Filho, J.L., Cavalcanti, A.Q., Converti, A., & Porto, A.L.P. (2009). Decolorization of synthetic dyes by basidiomycetes isolated from woods of the Atlantic Forest (PE), Brazil. *World Journal of Microbiology and Biotechnology*, 25 (8), 1499-1504. DOI: [10.1007/s11274-009-0034-2](https://doi.org/10.1007/s11274-009-0034-2)
- Mahajan, P., & Kaushal, J. (2020). Phytoremediation of azo dye methyl red by macroalgae *Chara vulgaris* L.: kinetic and equilibrium studies. *Environmental Science and Pollution Research*. 27, 26406–26418. DOI: [10.1007/s11356-020-08977-w](https://doi.org/10.1007/s11356-020-08977-w)
- Mahini, R., Esmaeili, H., & Foroutan, R. (2018). Adsorption of methyl violet from aqueous solution using brown algae *Padina sanctae-crucis*. *Turkish Journal of Biochemistry*, 43 (6), 623-631. DOI: [10.1515/tjb-2017-0333](https://doi.org/10.1515/tjb-2017-0333)
- Majhi, D. & Patra, B.N. (2020). Polyaniline and sodium alginate nanocomposite: a pH-responsive adsorbent for the removal of organic dyes from water. *RSC Advances*, 10 (71), 43904-43914. DOI: [10.1039/D0RA08125F](https://doi.org/10.1039/D0RA08125F)
- Marzbali, M.H., Mir, A.A., Pazoki, M., Pourjamshidian, R., & Tabeshnia, M. (2017). Removal of direct yellow 12 from aqueous solution by adsorption onto *Spirulina* algae as a high-efficiency adsorbent. *Journal of Environmental Chemical Engineering*, 5 (2), 1946-1956. DOI: [10.1016/j.jece.2017.03.018](https://doi.org/10.1016/j.jece.2017.03.018)
- Melo, B.C., Paulino, F.A.A., Cardoso, V.A., Pereira, A.G.B., Fajardo, A.R., & Rodrigues, F.H.A. (2018). Cellulose nanowhiskers improve the methylene blue adsorption capacity of chitosan-g-poly (acrylic acid) hydrogel. *Carbohydrate Polymers*, 181: 358-67. DOI: [10.1016/j.carbpol.2017.10.079](https://doi.org/10.1016/j.carbpol.2017.10.079)
- Mohammed, Y.M.M., & Mabrouk, M.E.M. (2020). Optimization of methylene blue degradation by *Aspergillus terreus* YESM 3 using response surface methodology. *Water Science & Technology*, 82 (10): 2007-2018. DOI: [10.2166/wst.2020.476](https://doi.org/10.2166/wst.2020.476)
- Nasoudari, E., Ameri, M., Shams, M., Ghavami, V., & Bonyadi, Z. (2020). The biosorption of Alizarin Red S by *Spirulina platensis*; process modelling, optimisation, kinetic and isotherm studies. *International Journal of Environmental Analytical Chemistry*. DOI: [10.1080/03067319.2020.1862814](https://doi.org/10.1080/03067319.2020.1862814)
- Naushad, M., Khan, A.M., Alothman Z.A., Khan, M.R., & Kumar, M. (2015). Adsorption of methylene blue on chemically modified pine nut shells in single and binary systems: isotherms, kinetics, and thermodynamic studies. *Desalination and Water Treatment*, 57 (34), 15848-15861. DOI: [10.1080/19443994.2015.1074121](https://doi.org/10.1080/19443994.2015.1074121)
- Omar, H., El-Gendy, A., & Al-Ahmary, K. (2018). Bioremoval of toxic dye by using different marine macroalgae. *Turkish Journal of Botany*, 42 (1), 15-27. DOI: [10.3906/bot-1703-4](https://doi.org/10.3906/bot-1703-4)
- Priyadarshini, E., Priyadarshini, S.S., & Pradhan, N. (2019). Heavy metal resistance in algae and its application for metal nanoparticle synthesis. *Applied Microbiology and Biotechnology*, 103 (8), 3297-3316. DOI: [10.1007/s00253-019-09685-3](https://doi.org/10.1007/s00253-019-09685-3)
- Radoor, S., Karayil, J., Parameswaranpillai, J., & Siengchin, S. (2020). Adsorption of methylene blue dye from aqueous solution by a novel PVA/CMC/halloysite nanoclay bio composite: Characterization, kinetics, isotherm and antibacterial properties. *Journal of Environmental Health Science and Engineering*. 18 (2), 1311-27. DOI: [10.1007/s40201-020-00549-x](https://doi.org/10.1007/s40201-020-00549-x)
- Radwan, E.K., Abdel-Aty, A.M., El-Wakeel, S.T., & Abdel Ghafar, H.H. (2020). Bioremediation of potentially toxic metal and reactive dye-contaminated water by pristine and modified *Chlorella vulgaris*. *Environmental Science and Pollution Research*, 27, 21777–21789. DOI: [10.1007/s11356-020-08550-5](https://doi.org/10.1007/s11356-020-08550-5)
- Renita, A.A., Vardhan, K.H., Kumar, P.S., Nguenagni, P.T., Abilarasu, A., Nath, S., Kumari, P., & Saravanan, R. (2021). Effective removal of malachite green dye from aqueous solution in hybrid system utilizing agricultural waste as particle electrodes. *Chemosphere*, 273, 129634. DOI: [10.1016/j.chemosphere.2021.129634](https://doi.org/10.1016/j.chemosphere.2021.129634)
- Shahyari, Z., Goharizi, A.S., & Azadi, M. (2010). Experimental study of methylene blue adsorption from aqueous solutions onto carbon nano tubes. *International Journal of Water Resources and Environmental Engineering*, 2 (2), 016-028.

- Shih, M.C. (2012). Kinetics of the batch adsorption of methylene blue from aqueous solutions onto rice husk: effect of acid-modified process and dye concentration. *Desalination and Water Treatment*, 37 (1-3), 200-214. DOI: [10.1080/19443994.2012.661273](https://doi.org/10.1080/19443994.2012.661273)
- Silva, F., Nascimento, L., Brito, M., da Silva, K., Paschoal, W., & Fujiyama, R. (2019). Biosorption of methylene blue dye using natural biosorbents made from weeds. *Materials (Basel)*, 12 (15), 2486. DOI: [10.3390/ma12152486](https://doi.org/10.3390/ma12152486)
- Soltani, R.D.C., Khorramabadi, G.S., Khataee, A.R., & Jorfi, S. (2014). Silica nanopowders/alginate composite for adsorption of lead (II) ions in aqueous solutions. *Journal of the Taiwan Institute of Chemical Engineers*, 45 (3):973-980. DOI: [10.1016/j.jtice.2013.09.014](https://doi.org/10.1016/j.jtice.2013.09.014)
- Soto-Ramirez, R., Lobos, M.G., Cordova, O., Poirrier, P., & Chamy, R. (2021). Effect of growth conditions on cell wall composition and cadmium adsorption in *Chlorella vulgaris*: A new approach to biosorption research. *Journal of Hazardous Materials*, 411, 125059. DOI: [10.1016/j.jhazmat.2021.125059](https://doi.org/10.1016/j.jhazmat.2021.125059)
- Sun, J., Dai, X., Wang, Q., van Loosdrecht, M.C.M., & Ni, B.J. (2019). Microplastics in wastewater treatment plants: Detection, occurrence and removal. *Water Research*, 152, 21-37. DOI: [10.1016/j.watres.2018.12.050](https://doi.org/10.1016/j.watres.2018.12.050)
- Tumin, N.D., Chuah, A.L., Zawani, Z., & Rashid, S.A. (2008). Adsorption of copper from aqueous solution by elais guineensis kernel activated carbon. *Journal of Engineering Science and Technology*, 3 (2): 180-189.
- Tural, B., Ertas, E., Enez, B., Agüloğlu Fincan, S., & Tural, S. (2017). Preparation and characterization of a novel magnetic biosorbent functionalized with biomass of *Bacillus subtilis*: Kinetic and isotherm studies of biosorption processes in the removal of Methylene Blue. *Journal of Environmental Chemical Engineering*, 5 (5):4795-4802. DOI: [10.1016/j.jece.2017.09.019](https://doi.org/10.1016/j.jece.2017.09.019)
- Üçüncü Tunca, E., Terzioğlu, K., & Türe, H. (2017). The effects of alginate microspheres on phytoremediation and growth of *Lemna minor* in the presence of Cd. *Chemistry and Ecology*, 33 (7):652-668. DOI: [10.1080/02757540.2017.1337102](https://doi.org/10.1080/02757540.2017.1337102)
- Venkataraghavan, R., Thiruchelvi, R., & Sharmila, D. (2020). Statistical optimization of textile dye effluent adsorption by *Gracilaria edulis* using Plackett-Burman design and response surface methodology. *Heliyon* 6 (10): e05219. DOI: [10.1016/j.heliyon.2020.e05219](https://doi.org/10.1016/j.heliyon.2020.e05219)
- Vijayaraghavan, K., Premkumar, Y., & Jegan, J. (2016). Malachite green and crystal violet biosorption onto coco-peat: characterization and removal studies. *Desalination and Water Treatment*, 57 (14): 6423-6431. DOI: [10.1080/19443994.2015.1011709](https://doi.org/10.1080/19443994.2015.1011709)
- Vu, H.C., Dwivedi, A.D., Le, T.T., Seo, S.H., Kim, E.J., & Chang, Y.S. (2017). Magnetite graphene oxide encapsulated in alginate beads for enhanced adsorption of Cr(VI) and As(V) from aqueous solutions: Role of crosslinking metal cations in pH control. *Chemical Engineering Journal*, 307, 220-229. DOI: [10.1016/j.cej.2016.08.058](https://doi.org/10.1016/j.cej.2016.08.058)
- Weber, W.J. (1972). *Physicochemical Processes: For Water Quality Control*, Wiley Interscience, NY.
- Xia, M., Zheng, X., Du, M., Wang, Y., Ding, A., & Dou, J. (2018). The adsorption of Cs(+) from wastewater using lithium-modified montmorillonite caged in calcium alginate beads. *Chemosphere*, 203, 271-280. DOI: [10.1016/j.chemosphere.2018.03.129](https://doi.org/10.1016/j.chemosphere.2018.03.129)
- Xu, T., Wang, X., Huang, Y., Lai, K., & Fan, Y. (2019). Rapid detection of trace methylene blue and malachite green in four fish tissues by ultra-sensitive surface-enhanced Raman spectroscopy coated with gold nanorods. *Food Control*, 106, 106720. DOI: [10.1016/j.foodcont.2019.106720](https://doi.org/10.1016/j.foodcont.2019.106720)
- Xu, Y.J., Tian, X.H., Zhang, X.Z., Gong, X.H., Liu, H.H., Zhang, H.J., Huang, H., & Zhang, L.M. (2012). Simultaneous determination of malachite green, crystal violet, methylene blue and the metabolite residues in aquatic products by ultra-performance liquid chromatography with electrospray ionization tandem mass spectrometry. *Journal of Chromatographic Science*, 50 (7): 591-597. DOI: [10.1093/chromsci/bms054](https://doi.org/10.1093/chromsci/bms054)
- Zhang, S., Wang, Z., Zhang, Y., Pan, H., & Tao, L. (2016). Adsorption of methylene blue on organosolv lignin from rice straw. *Procedia Environmental Sciences*, 31, 3-11. DOI: [10.1016/j.proenv.2016.02.001](https://doi.org/10.1016/j.proenv.2016.02.001)
- Zhao, M., & Liu, P. (2008). Adsorption behavior of methylene blue on halloysite nanotubes. *Microporous and Mesoporous Materials*, 112 (1-3), 419-424. DOI: [10.1016/j.watres.2009.10.042](https://doi.org/10.1016/j.watres.2009.10.042)